Changes of Tropical Precipitation Efficiency under Global Warming Projected by CMIP5 Model Simulations

HSIAO-WEI LIU [1] and JIA-YUH YU [2]

[1] ***National Science and Technology Center for Disaster Reduction, New Taipei City, Taiwan, R.O.C.***

[2] ***Department of Atmospheric Sciences, National Central University, Taoyuan City, Taiwan R.O.C.***

Abstract

Future changes of tropical precipitation efficiency (PE) are analyzed using model simulation outputs from the Coupled Model Intercomparison Project phase 5 (CMIP5) with the representative concentration pathway 8.5 (RCP8.5) scenario. Under global warming, the tropical moisture increases relatively homogeneously with a rate of approximately ~7 $\%K^{-1}$ during the period from 2006 to 2099, consistent with the Clausius-Clapeyron (C.-C.) scaling. In contrast to moisture changes, however, precipitation changes exhibit strong regional discrepancies with the coexistence of positive and negative precipitation trends (e.g., positive trend over ITCZ and negative trend elsewhere), which implies a decrease of the precipitation efficiency under global warming when the tropic is considered as a whole.

A budget analysis of the PE equation shows that PE has decreased in both climatologically ascending and descending regions due to the general weakening of tropical circulation (convection) under global warming. However, we also find a very unique feature of precipitation changes in the equatorial Eastern Pacific in which changes of precipitation are far beyond the C.-C. scaling, which is worth further studying in the future

1. Introduction

Changes in the large-scale water cycle are an expected consequence of anthropogenic climate change. As the climate warms, water-holding capacity increases with higher temperatures (Trenberth et al. 2003). The atmospheric water vapor shows a robust increase as relative humidity remains relatively unchanged. Held and Soden (2006) used the CMIP3 archive to look for robust responses of the water cycle to global warming. It is estimated that thermodynamic relationship between warming and moisture is generally determined according to the Clausius–Clapeyron relation, For example, Wentz et al. (2007) estimated the increased rate of atmospheric moisture in 1987–2006 of approximately 7% in response to surface warming. However, observations and climate model simulations showed an increased rate of global-mean precipitation of 1%–3% in response to surface warming over the same period (Allen and Ingram 2002; Held and Soden 2006).

Thus, we would expect higher precipitation under a warming climate assuming that water vapor eventually becomes precipitation. Research on precipitation change associated with a warming climate shows that wetter places become wetter and drier places become drier, based on both data records and climate model projections (Chou et al. 2009; Trenberth, 2011; Trenberth and Shea, 2005).

Precipitation efficiency is an important physical parameter in convective systems. The definitions of precipitation efficiency from these should be similar. The precipitation efficiency has been defined in water vapor related surface rainfall budget (LSPE) derived from water vapor and cloud budgets and in cloud microphysical budget (CMPE) derived from the microphysical budgets of cloud species (Li et al. 2002; Sui et al. 2007) and total precipitation divided by atmospheric total precipitable water (PW) during the same time period and at the same location (Tuller, 1973).

Understanding how the tropical atmosphere might change in response to anthropogenic global warming has increasingly become an important subject in climate studies.

In this study, we reexamine tropical regional precipitation efficiency (PE) changes based on modern climate model simulation outputs archived in CMIP5 (Taylor et al. 2012). Section 2 introduces the data and methodology used in this study. Section 3 mlti-model ensemble results. Major findings and suggestions are concluded in section 4.

2. Data and methodology

The data used in this study include monthly mean fields of specific humidity and temperature during the period 2006-2099 from the CMIP5 model simulation outputs for the representative concentration pathway 8.5 (RCP8.5) experiments downloaded from the Earth System Grid (https://pcmdi9.llnl.gov/projects/cmip5/). To facilitate the analysis, all climate model data are re-gridded to a common resolution of $2.5^o \times 2.5^o$, with 15 pressure levels from 1000 to 10hPa.

A modified definition of precipitation efficiency (PE) is proposed based on either cloud microphysics precipitation efficiency (CMPE) or water cycling processes including water vapor and hydrometeor species [large-scale precipitation efficiency (LSPE)] (Sui et al. 2007). It is found that the properly defined *PEs* include all moisture and hydrometeor sources associated with surface rainfall processes so that they range from 0% to 100%.

In this study, the precipitation efficiency *(PE)* of tropical atmosphere is defined as:

$$PE = \frac{Mq}{<q>} \qquad \textbf{(1)}$$

where *Mq* is a smoothly-posed physical quantity termed as the "gross moisture stratification"—a measure of moisture available for convective condensation (Yu et al. 1998). Physically, *Mq* can be regarded as the fraction of water vapor in the atmosphere that can be converted into precipitation subject to moist adiabatic adjustment or, in practice the "precipitation potential" of tropical atmosphere in presence of the large-scale wind convergence. For consistency, the specific humidity *q* is also in energy units by absorbing the latent heat per unit mass ($L = 2.5 \times 10^6 \, JKg^{-1}$).

The brackets in (1) represent a mass integration over the entire troposphere from P_T =100 *hPa* to P_o =1000 *hPa* , which is defined as

$$\langle \ \rangle = g^{-1}\int_{P_o}^{P_T}(\ )\mathrm{dp} \qquad \textbf{(2)}$$

where *g* is the gravitational constant.

The fractional change of *PE* can be estimated by:

$$\frac{PE'}{\overline{PE}} * T'^{-1}(\%K^{-1}) = (\frac{Mq'}{\overline{Mq}} - \frac{q'}{<\overline{q}>} - \frac{q'Mq'}{<\overline{q}>\overline{Mq}}) * T'^{-1}(\%K^{-1}) \qquad \textbf{(3)}$$

where $\overline{(\ )}$ denotes the climatology averaged over the entire data period from 2006 to 2099 and $(\ )'$ represents anomaly (or perturbation) between the two periods:2006-2015 and 2090-2099. All the term in units ($\%K^{-1}$) for air temperature anomalous. Other variables are calculated 15 models.

The terms on right hand side of (3) represents all the contributing effects responsible for the *PE* anomaly, including the anomalous convective condensation potential ($Mq'/\overline{Mq}$), the anomalous water vapor in atmosphere ($q'/\overline{q}$).The last term denotes contributions from anomalous mechanisms terms. Under the global warming, the atmosphere can accommodate changes in water vapor conditions, the second terms on right hand side is a negative contribution. In the following analysis, multi-model means of the 15 CMIP5 models outputs are taken in the budget analysis, focusing on the tropical oceanic domain (20°N-20°S) to avoid complexity caused by land topography.

3. Multi-model ensemble results

Figure 1 shows the climatology of *Mq* distribution as estimated from the CMIP5 models. The pattern of *Mq* is strongly influenced by the ocean surface conditions such that it closely follows the SST distribution (Yu et al. 1998). Larger values of its magnitude tend to occur over warmer SST areas. We also found that *Mq* and *PE* in the space showed a high correlation. Larger values of *PE* areas (contours) magnitude tend to occur over large of *Mq*. The *PE* magnitude ranges from 5 to 6% in the domain of interest.

Figure 2 shows the yearly changes of water vapor *(q)* and *Mq* during the period from 2006 to 2099 projected by the multi-model mean of 15 CMIP5 models over the tropical regions. The CMIP5 models dataset for this study in Table 1. It is found that, over the tropical region, water vapor *(q)* increases by about 20% (12.23 to 15.24 $10^3 \, JKg^{-1}$) over the period 2006-2099. Since the multi-model mean tropical surface warming projected by the RCP8.5 experiments is about $3\,^oC$ over the same period, this corresponds to approximately 7% increase in water vapor *(q)* per unit ^oC of atmospheric warming, consistent with the estimates from the Clausius–Clapeyron equation for the saturation vapor pressure (Held and Soden 2006).

In contrast, *Mq* has no significant increase in water vapor. If one views the ratio of *Mq* over water vapor (i.e., *Mq/<q>*) as a measure of precipitation efficiency, a smaller value of *Mq/<q>* implies a less efficiency in producing precipitation. As shown in Fig. 2 (see green curves), while trends of *Mq/<q>* consistently decreasing under global warming (ranging from 0.043 in 2006 to 0.0419 in 2099). This means that a large portion of the increased water vapor must be contained in the atmosphere as the moisture-holding capacity of atmosphere largely enhances in a warmer condition (Stephens and Ellis 2008)

To further understand the spatial distribution of *PE* under global warming. Figure 3 display the spatial distribution of fractional change of *PE*, which its differences between averages of 2090-2099 and 2006-2015(in units of $\%K^{-1}$). We are found that over the mean ascending or descending region show consistently decreasing fractional change of *PE* under global warming. The values is about -2.24($\%K^{-1}$) and -2.28($\%K^{-1}$), respectively.

One particular example occurs in the eastern Pacific ITCZ where precipitation efficiency anomalies are mostly positive under global warming. We will discuss in section 4. To further explore the mechanisms responsible for regional discrepancies of *PE* anomalies under global warming in the tropics. The term budget results over the aforementioned domains are displayed in Figure 4. Over the tropical area, the negative precipitation efficiency (see Fig. 4) appear to come mainly from the strengthening of anomalous water vapor in atmosphere ($q'/\overline{q}$), which is referred to as the thermodynamic effect, this means the moisture-holding capacity of atmosphere largely enhances in a warmer condition (Stephens and Ellis 2008). While the first term ($Mq'/\overline{Mq}$) has a counteracting effect.

One particular example occurs in the eastern Pacific ITCZ where precipitation efficiency anomalies are mostly positive even though the mean vertical motion are descending there (see Fig. 3).Further explore the mechanisms responsible for regional discrepancies of *PE* anomalies in eastern Pacific (see Fig. 5). In contrast to the tropical area, the positive precipitation efficiency appear to come strongly mainly from the anomalous convective condensation potential ($Mq'/\overline{Mq}$) this means the anomaly of gross moisture stratification (*Mq*) enhances in eastern Pacific.

4. Conclusion

Future tropical precipitation efficiency changes are investigated based on the multi-model means of 15 CMIP5 models outputs for the RCP8.5 scenario. This study shows that, while decreases in *PE* are relatively homogeneous in space, except to the eastern Pacific.

A term budget analysis of the *PE* equation suggests that changes of tropical precipitation efficiency are controlled mainly by the thermodynamic effect ($q'/\overline{q}$), this means the moisture-holding capacity of atmosphere largely enhances in a warmer condition. We now explain the cause of the positive of the precipitation efficiency in the eastern Pacific region. In the *PE* analysis, over the eastern Pacific, we found that the first term ($Mq'/\overline{Mq}$) contributions are particularly larger than in tropical region.

Under global warming, gross moisture stratification (*Mq*) should change. The anomalous *Mq* can be written as

$$Mq' = \left\langle \Omega' \partial_p \overline{q} \right\rangle + \left\langle \overline{\Omega} \partial_p q' \right\rangle + residual \qquad \textbf{(4)}$$

Where Ω is a tropical vertical profile of vertical motion for deep convection. In this study, Ω is obtained by using Eq. (2.2a) in Yu et al. (1998), the specific humidity *q*.

Based on (4), we evaluated the contribution from changes *Mq*. Since *Mq* depends on changes in moisture *q*, which is usually positive since most anomalous moisture concentrates in the lower troposphere under global warming. In summary, we want unified anomalous *Mq* which all terms are in energy units ($\%K^{-1}$).The anomalous *Mq* will be written as:

$$\frac{Mq'}{\overline{Mq}} = \frac{\left\langle \Omega' \partial_p \overline{q} \right\rangle}{\overline{Mq}} + \frac{\left\langle \overline{\Omega} \partial_p q' \right\rangle}{\overline{Mq}} + residual \qquad \textbf{(5)}$$

Mq changes in the tropics are controlled mainly by the thermodynamic effect ($\left\langle \overline{\Omega} \partial_p q' \right\rangle$) no matter over the tropical (see fig. 6a) or eastern Pacific regions (see fig. 6b). Particular attention to the dynamics effect ($\left\langle \Omega' \partial_p \overline{q} \right\rangle$) in the eastern Pacific region is higher than the tropical region, which means an enhanced upward motion in this regions under global warming. The precipitation changes seem to comply more with the "warmer-get-wetter" mechanism, especially over the equatorial eastern Pacific.

Acknowledgments.

This work was sponsored by the Ministry of Science and Technology (MOST) under Grants MOST 105-2811-M-008-056.The authors thank the CMIP5 climate modeling groups for producing and making available their model simulation outputs. The CMIP5 data were downloaded from the Earth System Grid at the Lawrence Livermore National Laboratory, Department of Energy, USA (https://pcmdi9.llnl.gov/projects/cmip5/).

References

Allen, M. R., and W. J. Ingram, 2002: Constraints on future changes in the hydrological cycle, Nature, 419, 224–228.

Chou, C., J. D. Neelin, C.-A. Chen, and J.-Y. Tu, 2009: Evaluating the ‘‘rich-get-richer’’ mechanism in tropical precipitation change under global warming. J. Climate, 22, 1982–2005.

Held, I. M., and B. J. Soden, 2006: Robust responses of the hydrological cycle to global warming, J. Climate, 19, 5686–5699.

Li, X., C.-H Sui, and K.-M Lau, 2002: Precipitation efficiency in the tropical deep convective regime: a 2-D cloud resolving modeling study. J Meteorol Soc Jpn 80,205–212

Stephens, G. L., and T. D. Ellis, 2008: Controls of global mean precipitation increases in global warming GCM experiments, J. Climate, 21, 6141–6155.

Sui, C.-H., X. Li, and M.-J. Yang, 2007: On the definition of precipitation efficiency. J. Atmos. Sci., 64, 4506–4513

Taylor, K. E., J. S. Ronald, and G. A. Meehl, 2012: An overview of CMIP5 and the experiment design. Bull. Amer. Meteor. Soc., 93, 485–498, doi:10.1175/BAMS-D-11-00094.1.

Trenberth, K. E. 2011: Changes in precipitation with climate change. Clim. Res., 445(47), 123–138.

_____., A. Dai, R. M. Rasmussen, and D. B. Parsons, 2003: The changing character of precipitation. Bull. Amer. Meteor. Soc., 84, 1205-1217.

_____., and D. J. Shea, 2005: Relationships between precipitation and surface temperature, Geophys. Res. Lett., 32, L14703, doi:10.1029/2005GL022760.

Tuller, S. E., 1973: Seasonal and annual precipitation efficiency in Canada, Atmosphere, 11(2), 52–66.

Yu J.-Y., C. Chou and J. D. Neelin, 1998：Estimating the gross moist stability of the tropical atmosphere. J. Atmos. Sci., 55, 1354-1372.

Wentz, F.J., Ricciardulli, L., Hilburn, K. and Mears, C. 2007: How much more rain will global warming bring? Science, 317, 233-235.

Table 1: A list of 15 coupled climate models in the CMIP5 archive used in this study.

Model Name	Modeling Center (or Group)
ACCESS1.0	Commonwealth Scientific and Industrial Research Organization (CSIRO) and Bureau of Meteorology (BOM), Australia
BCC-CSM1.1	Beijing Climate Center, China Meteorological Administration
CanESM2	Canadian Centre for Climate Modelling and Analysis
CCSM4	National Center for Atmospheric Research
CESM1(BGC)	Community Earth System Model Contributors
CNRM-CM5	Centre National de Recherches Meteorologiques/Centre Europeen de Recherche et Formation Avancee en Calcul cientifique
FIO-ESM	The First Institute of Oceanography, SOA, China
GFDL-CM3	NOAA Geophysical Fluid Dynamics Laboratory
HadGEM2-CC	Met Office Hadley Centre (additional HadGEM2-ES realizations contributed by Instituto Nacional de Pesquisas Espaciais)
IPSL-CM5A-MR	Institut Pierre-Simon Laplace
MIROC-ESM	Japan Agency for Marine-Earth Science and Technology, Atmosphere and Ocean Research Institute (The University of Tokyo), and National Institute for Environmental Studies
MIROC5	Atmosphere and Ocean Research Institute (The University of Tokyo), National Institute for Environmental Studies, and Japan Agency for Marine-Earth Science and Technology
MPI-ESM-LR	Max-Planck-Institut für Meteorologie (Max Planck Institute for Meteorology)
MRI-CGCM3	Meteorological Research Institute
NorESM1-M	Norwegian Climate Centre

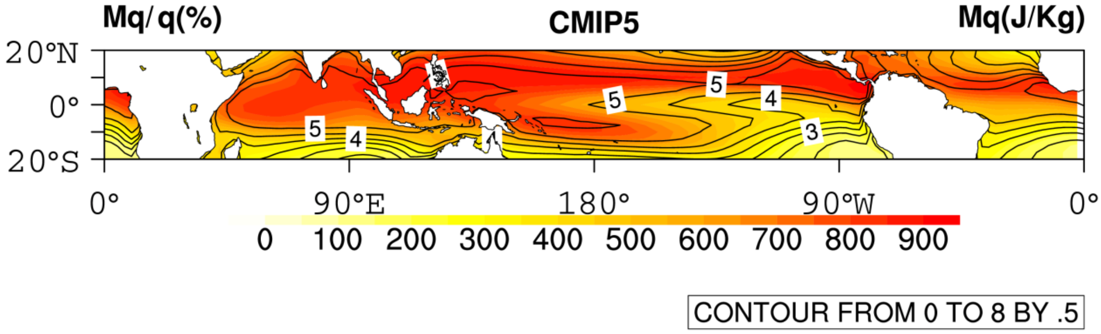

Figure 1: Spatial patterns of Gross Moisture Stratification (Mq, color shadings) derived from 15 CMIP5 models under the RCP8.5 scenario over the period 2006~2099(contours, in ratio between Mq and water vapor (q) in units of %).

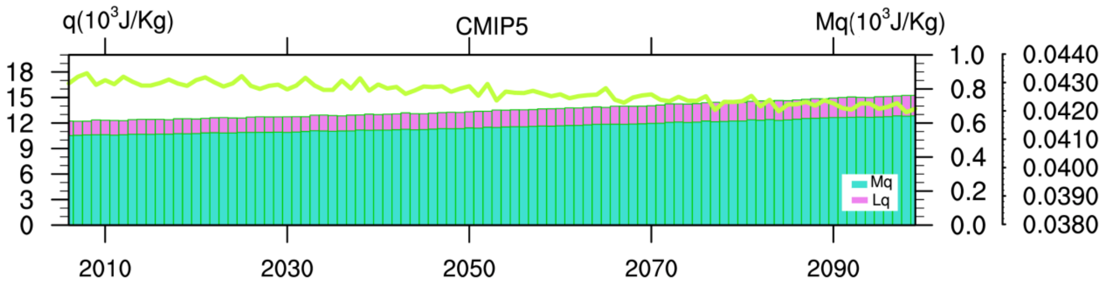

Figure 2: The yearly time series of water vapor (red, in unit of $10^3 JKg^{-1}$) and Mq (green, in unit of $10^3 JKg^{-1}$) derived from the multi-model means of 15 CMIP5 models under the RCP8.5 scenario over the period 2006~2099. The ratio between Mq and water vapor [green line, in day^{-1}] is also displayed to highlight changes of precipitation effectiveness under global warming.

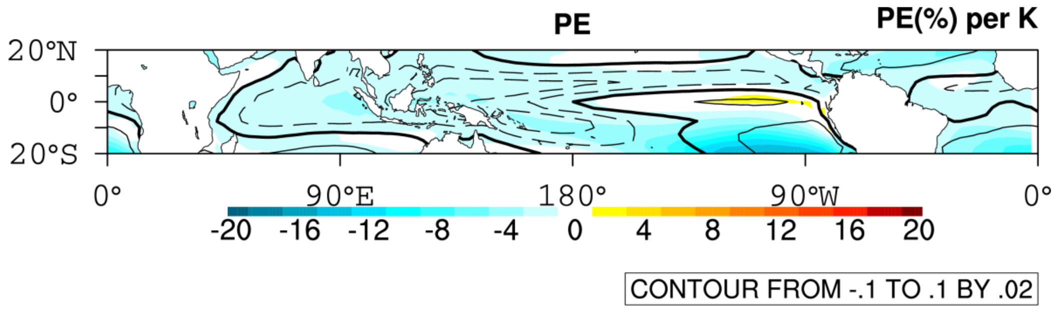

Figure 3: Spatial patterns of precipitation efficiency changes derived from 15 CMIP5 models output over the period 2006~2099(color shadings, in units of $\%K^{-1}$). The thick solid lines denote the $\overline{\omega}_{500} = 0$ contours which separate the mean ascending region from the descending region.

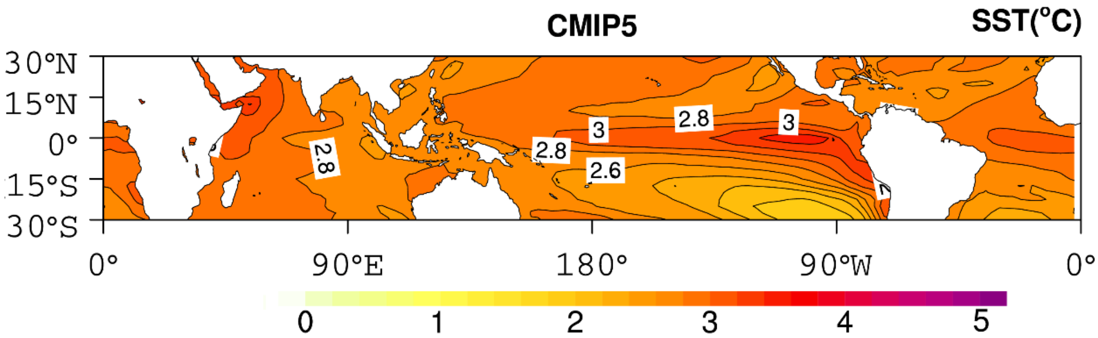

Figure 4: Spatial pattern of SST warming (in ℃) between the two period 2006-2015 and 2090-2099 simulated by a multi-model mean of 15 CMIP5 models under the RCP8.5 scenario.

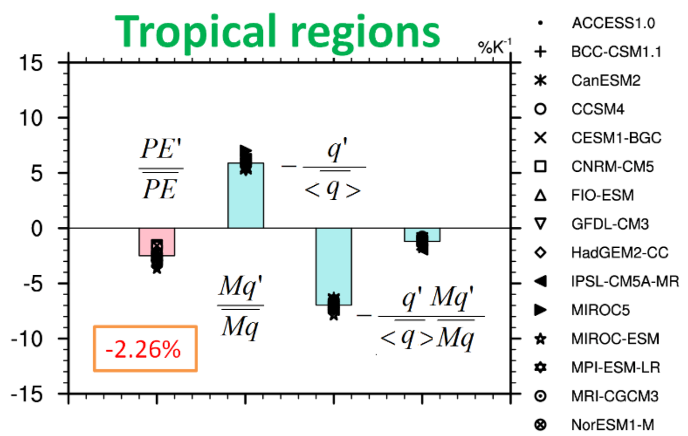

Figure 4: Term budget results for the precipitation efficiency over the tropical (20S~20N) differences between averages of 2090-99 and 2006-2015. All terms are in units ($\%K^{-1}$)

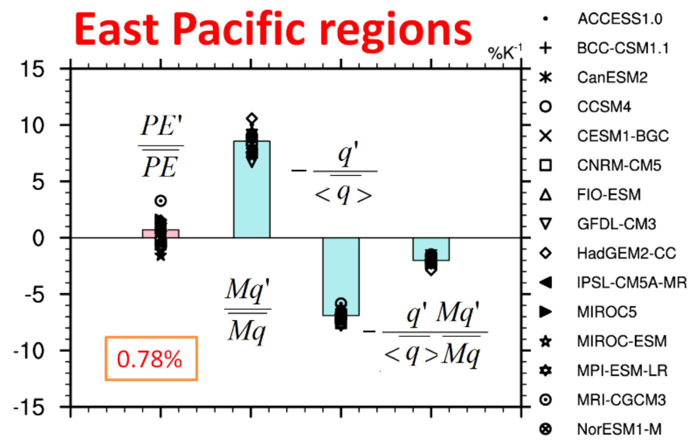

Figure 5: Similar to the Figure 4 but over the East Pacific regions (5S~5N, 120~90W)

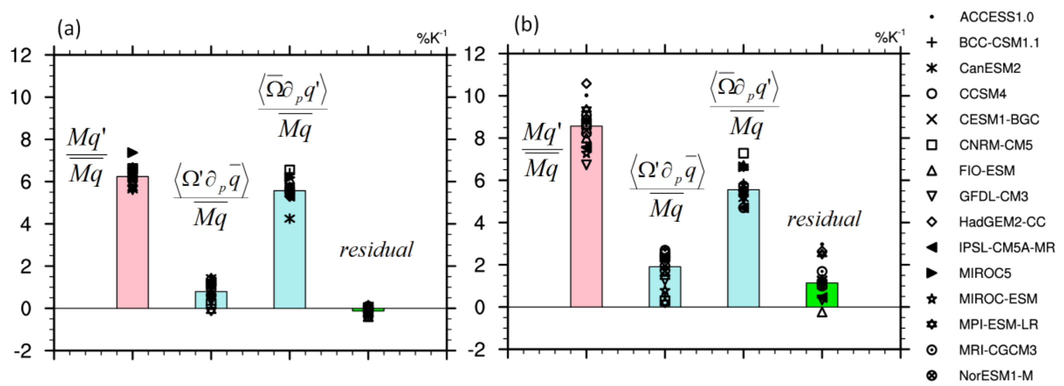

Figure 6: Term budget results for the Mq anomalies over the (a) tropical region (20S~20N), (b) over the East Pacific regions (5S~5N, 120~90W). All terms are in energy units ($\%K^{-1}$).